

See discussions, stats, and author profiles for this publication at: <https://www.researchgate.net/publication/225033663>

Characterization of Comb-Shaped Polymers Using GPC–Multidetector Method

ARTICLE · AUGUST 1999

CITATIONS

4

READS

43

2 AUTHORS:



[Wolfgang Radke](#)

PSS Polymer Standards Service

60 PUBLICATIONS **792** CITATIONS

SEE PROFILE



[Axel H E Mueller](#)

Johannes Gutenberg-Universität Mainz

590 PUBLICATIONS **17,860** CITATIONS

SEE PROFILE

Synthesis and Characterization of Comb-Shaped Polymers by SEC with On-Line Light Scattering and Viscometry Detection

Wolfgang Radke*,† and Axel H. E. Müller‡

Deutsches Kunststoff-Institut (German Institute for Polymers), Schlossgartenstr. 6,
D-64289 Darmstadt, Germany, and Macromolecular Chemistry II, Universität Bayreuth,
D-95440 Bayreuth, Germany

Received October 26, 2004; Revised Manuscript Received January 31, 2005

ABSTRACT: Comb-shaped polystyrenes with UV-labeled side chains were synthesized and analyzed by SEC with on-line light scattering and viscometry detection. The introduction of the UV label allows for a model-independent determination of the number of grafts within each SEC slice and therefore the calculation of the expected contraction factors, $g = \langle R_{g,br}^2 \rangle / \langle R_{g,lin}^2 \rangle$ and $g' = [\eta]_{br} / [\eta]_{lin}$. Using molecular weight sensitive detectors, the contraction factors were determined experimentally and compared to the expected ones. It was found that the experimentally determined g values are larger than the ones calculated on the basis of the Gaussian chain assumption. Therefore, the calculation of the number of branches based on theoretically expected contraction factors is not feasible. Attempts to include corrections for excluded-volume effects failed. For the exponent ϵ of the relationship $g' = g^\epsilon$ a value close to $\epsilon = 1$ was found, in contradiction with the expectations from the Flory–Fox and Zimm–Kilb relations. It was observed that the intrinsic viscosities of the combs are close to the intrinsic viscosities of the parent backbone polymer itself, allowing to use this empirical relationship for the determination of the amounts of grafts present in the polymer.

Introduction

Branched polymers have attracted attention from both a scientific and a commercial point of view. The introduction of branches results in a reduction of the melt viscosity and, thus, in an improved processability without loss in mechanical properties. Branching leads to a contraction of the molecules relative to the size of the linear analogues of same molecular weight. Zimm and Stockmayer have first treated this contraction effect theoretically in 1949.¹ They defined a contraction factor, $g = \langle R_{g,br}^2 \rangle / \langle R_{g,lin}^2 \rangle$, as the ratio of the mean-squared radii of gyration of the branched and linear molecule having the same molecular weight. On the basis of the assumption of Gaussian chains, they derived equations for g for a variety of branched structures including stars and regularly and randomly branched polymers. Since then, contraction factors have been calculated for other topologies by various authors.^{2–6} Even more than 50 years later, branching analysis is still mainly done on the basis of the Zimm–Stockmayer theory. However, the difficulties arising from the determination of mean-squared radii by light scattering frequently led to the use of intrinsic viscosity data, which can be obtained more easily. In analogy to the definition of the contraction factor g , a contraction factor $g' = [\eta]_{br} / [\eta]_{lin}$ can be defined as the ratio of the intrinsic viscosities of the branched and linear molecule at same molecular weight. On the basis of the Flory–Fox equation, which relates the intrinsic viscosity to the radius of gyration, a relationship of the form $g' = g^\epsilon$ with $\epsilon = 3/2$ was proposed.⁷ However, Zimm and Kilb derived at a value of $\epsilon = 1/2$ for star polymers and assumed this value to be universal.⁸ According to Berry, a simple power law cannot describe the relation between g' and g .^{2,9} Until today, the value of the parameter ϵ is still under dispute,

even for the simplest branched structures, the star polymers. Theoretical treatments and computer simulations continue to clarify the effects of solvent quality on the chain extension in various solvents.^{10–21}

Beside the difficulties related with the theory of branched polymers, problems were also found with the experimental determination of the contraction factors g and g' . The determination requires comparing the radii of gyration or intrinsic viscosities of branched and linear polymers having the same molecular weight. However, for synthetic polymers we have to take into account their polydispersity. Studies of the contraction factors therefore have been performed mostly on polymers prepared by living polymerization techniques. As an alternative, tedious fractionation procedures were used to obtain polymers with narrow molecular weight distribution. However, such procedures can be used for the synthesis of model polymers but are not applicable for the characterization of branched polymers in industries.

In the recent years molecular weight sensitive SEC detectors have become popular. On-line light scattering detectors allow for the determination of molecular weight and radius of gyration for samples, which have been fractionated by SEC into nearly monodisperse slices.^{22–24} Viscosity detectors allow the determination of the intrinsic viscosity of the eluting fraction^{25–28} and—via universal calibration²⁹—the determination of its molecular weight. Besides the molecular weight of the eluting species, both methods yield the size information on the branched molecule required for the determination of the contraction factors g and g' . Therefore, SEC with on-line molecular weight sensitive detection is assumed to be the method of choice for the characterization of branched polymers. However, SEC is performed in good solvents, while the theoretical calculation of contraction factors for different structures is performed using Gaussian coil approximation, which should resemble more closely θ -conditions.

† Deutsches Kunststoff-Institut.

‡ Universität Bayreuth.

* Corresponding author. E-mail wradke@dki.tu-darmstadt.de.

In the present study we are investigating the ability of SEC with light scattering and viscometry detection for the characterization of comb-shaped polymers. The polymers are composed of side chains having a narrow molecular weight distribution, while for the backbone polymers with narrow or broad molecular weight distribution were chosen. This allows for a comparison of well-defined (narrowly distributed) comb polymers with those having a broad molecular weight distribution, which should more closely resemble polymers from real industrial processes. Thus, it is possible to compare the capabilities of SEC with molecular weight sensitive detectors for model polymers and real-life samples. The branched polymers were UV-labeled in the side chains, which allows for the determination of the weight fraction of side chains within each SEC slice. Thus, it can be proven whether the assumption of a homogeneous side chain distribution is fulfilled. Having determined the number of side chains within each SEC slice, it is possible to calculate the contraction factors, g or g' , on the basis of existing theories and to compare these to the ratios determined experimentally using on-line light scattering or viscometry detection, respectively.

Experimental Part

Synthesis of Comb-Shaped Polymers with UV-Labeled Side Chains. The comb polymers were prepared by grafting living poly(*p*-methylstyrene) anions onto a partially brominated poly(*p*-methylstyrene) backbone. The synthetic route for the polymers is given in Scheme 1. The introduction of the phenanthrene label was realized using 1-phenanthryl-1-phenylethylene (PPE), which was prepared according to the literature.³⁰

The synthesis of the polymer backbone having narrow molecular weight distribution was performed by anionic polymerization in cyclohexane at 40 °C using standard procedures. The backbone with broad molecular weight distribution was synthesized by slowly adding in parallel a solution of diphenylhexyllithium and a solution of *p*-methylstyrene to THF at room temperature. With every addition of initiator new chains will be produced giving rise to a broadening of the molecular weight distribution. The maximum polydispersity that can be obtained by this procedure is limited to a polydispersity of 2, however.³¹ The polymers obtained were precipitated into a large excess of methanol and dried in a vacuum.

The bromination of the backbone polymers was performed in cyclohexane solution. In a typical experiment 1 g of poly(*p*-methylstyrene) was dissolved in 10 g of cyclohexane together with 199 mg (1.12 mmol) of *N*-bromosuccinimide (NBS) and 7.5 mg (0.04 mmol) of benzoyl peroxide (BPO). After degassing by repeated freeze–thaw cycles the solution was heated to 60 °C for 3–4 h. The succinimide was removed by filtration, and the solvent was stripped off. After redissolving the polymer in THF, it was precipitated into a large excess of methanol and dried in a vacuum. It should be noted that only approximately 50% of the desired degree of bromination was achieved, as indicated by ¹H NMR spectroscopy.

The synthesis of the living precursor side chains was performed in 30 wt % solution of *p*-methylstyrene in cyclohexane. In a typical experiment 5 g of *p*-methylstyrene (42.3 mmol) and 16.7 g of cyclohexane were weighed into a glass ampule sealed with a Teflon stopcock. The solution was carefully degassed by repeated freeze–thaw cycles. The monomer solution was titrated in an inert atmosphere with *sec*-butyllithium until a pale yellow color was persistent. Then 0.36 mL of 1.7 *m sec*-butyllithium was added via syringe in a glovebox. The solution was reacted at 40 °C for 2 h. After completion of the polymerization a small excess of 189 mg (0.67 mmol) of PPE was dissolved 49 mL of THF. Impurities were removed by titrating the PPE solution at room temperature

with *n*-butyllithium until a faint blue color was observed. The PPE solution was added to the living poly(*p*-methylstyrene). Upon addition a change from the orange color of the living poly(*p*-methylstyrene) anions to the dark blue color of the end-functionalized living chain ends was observed. SEC analysis of the reaction product yielded $M_n = 9100$ g/mol and a polydispersity of 1.08, in good agreement with the expected molecular weight. The living solution of the anions was kept at low temperature until used for the coupling procedure.

For the coupling reaction the brominated backbone was dissolved in dry THF at a concentration not exceeding 1 wt %. Higher concentrations led to gel formation during the coupling reaction. After carefully degassing, the labeled living poly(*p*-methylstyrene) anions were slowly added at room temperature, until a faint greenish color was persistent over 10 min. The reaction was terminated using methanol. Finally, the polymer was recovered by precipitation into a large excess of methanol.

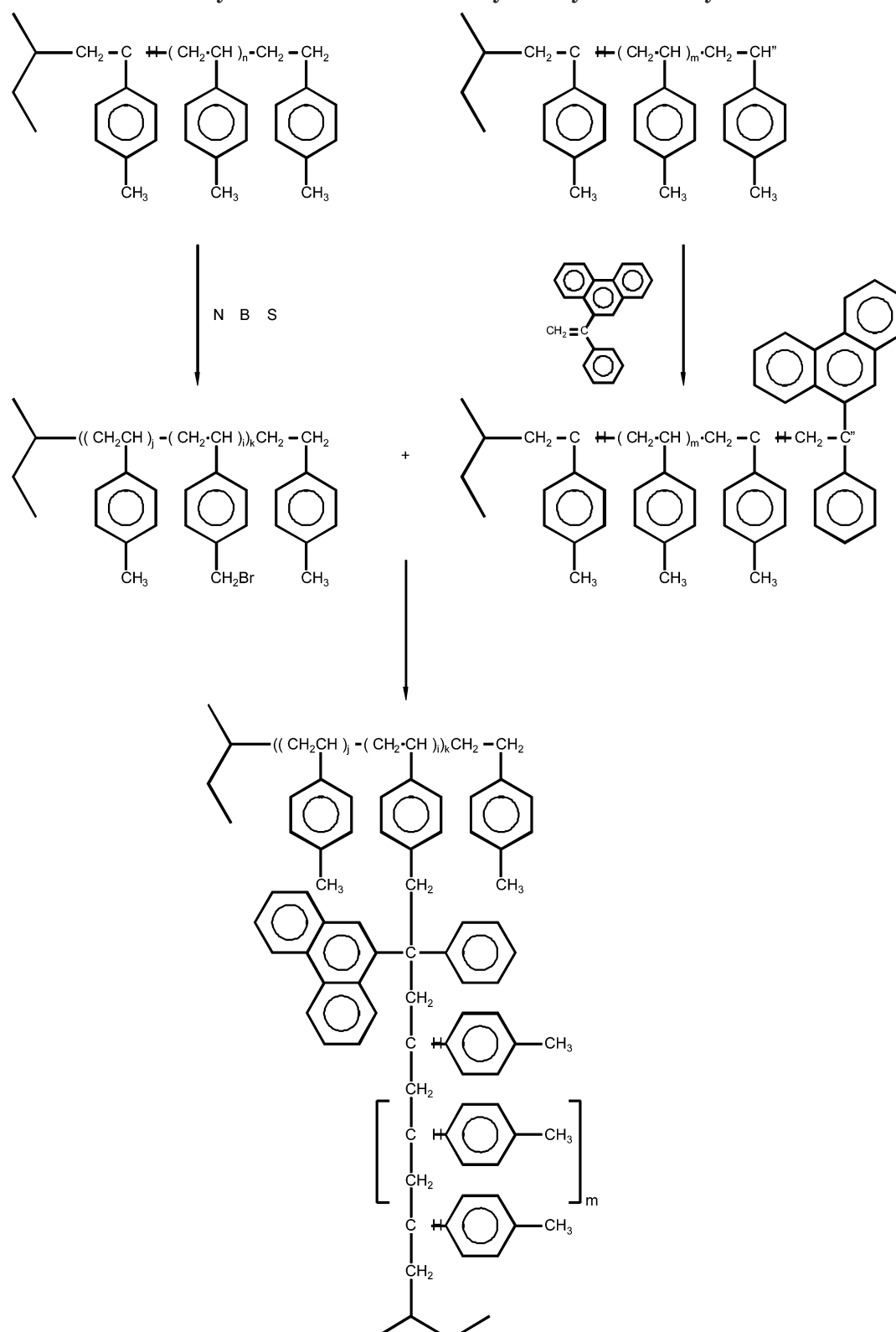
Characterization. SEC analyses were performed in THF at 0.5–1 mL/min using 5 μ PSS SDV columns (10^3 , 10^5 , 10^6 Å, 30×0.8 cm each). An Applied Biosystems S1000 UV diode array and a Bischoff 8110 RI detector were used. A Viskotek H502 B and/or a Wyatt Technology DAWN-F multiangle light scattering detector could be added. Data acquisition was performed using PSS WinGPC and Wyatt Technology WinAstra software. The injected amounts and flow rates were adjusted depending on the molecular weights and polydispersities of the samples.

For conventional SEC experiments toluene was used as an internal flow marker to correct for flow rate fluctuations. SEC calibrations were performed using a series of narrowly and broadly distributed poly(*p*-methylstyrene)s synthesized in our laboratory.

The multidetector setup is sensitive to band broadening and errors in the determination of delay volumes. This is especially important for samples having a narrow molecular weight distribution. Therefore, these samples were analyzed only in terms of weight-average molecular weight, weight-average intrinsic viscosity, and composition because these characteristics are obtained by integration over the complete peaks and are therefore not influenced by the problems mentioned. The different dependences of the RI and light scattering or viscosity detectors on molecular weight present another problem. While the RI signal is proportional to concentration, the signal of the light scattering and viscosity detector increase with molecular weight. As a consequence, the RI loses its sensitivity at the high molecular weight tail of the chromatogram, while the opposite is true for the light scattering and viscosity detectors. Therefore, the results in the tails of the chromatograms are less accurate than at the center of the chromatograms. In the present investigation additional problems arose from the use of different software packages for data acquisition of viscometric and UV data on the one hand and light scattering data on the other. While the WinGPC software uses the retention time at the UV detector as reference and corrects the elution volume for flow rate variations using an internal flow marker, the WinAstra software uses the retention time at the light scattering instrument as reference time and used no flow correction. A self-written routine was used to merge the data acquired by the different software packages and to correct for these problems.

The light scattering instrument was calibrated using pure toluene assuming a Rayleigh ratio of $14.06 \times 10^{-6} \text{ cm}^{-1}$ at 633 nm.³² The exact injection volume of the fixed autosampler loop was determined gravimetrically by filling the loop repeatedly with distilled water. The refractive index increment, dn/dc , of poly(*p*-methylstyrene) was estimated from the response of the RI detector. To do so, the detector response was calibrated with polystyrene standards using the known $dn/dc = 0.184 \text{ cm}^3/\text{g}$.³³ Assuming the dispersions of polystyrene and poly(*p*-methylstyrene) to be very similar, an average value of $dn/dc = 0.170 \text{ cm}^3/\text{g}$ was found from the relative responses of a variety of poly(*p*-methylstyrene)s. However, since the refractometer uses a different wavelength than the light-scattering

Scheme 1. Synthesis of Model Comb Polymers by Anionic Polymerization



instrument, the dn/dc value was cross-checked for three samples using a scanning interferometer operated at a wavelength of 633 nm. These determinations resulted in good agreement with the value found from the refractive index detector.

Determination of the composition of the comb polymers was performed for the individual slices in the following way. After suitable calibration of the detector responses for the labeled and nonlabeled poly(*p*-methylstyrene)s, the composition was calculated assuming additivity of the re-

sponses of the individual components.

$$A_{c,i}(\lambda) = c_i[w_{sc,i}\epsilon_{sp,sc}(\lambda) + (1 - w_{sc,i})\epsilon_{sp,bb}(\lambda)] \quad (1)$$

where $A_{c,i}(\lambda)$ is the absorption of slice i , for the wavelength λ . c_i and $w_{sc,i}$ are the polymer concentration and the weight fraction of side chains within the slice. $\epsilon_{sp,sc}$ and $\epsilon_{sp,bb}$ are the specific absorption coefficients for side chains and backbone, respectively. By using at least two different wavelengths, which differ in their specific absorption coefficient for side

Table 1. Characterization Data of Linear Poly(*p*-methylstyrene)s

sample	$M_w/10^4$	M_w/M_n	$[\eta]/\text{cm}^3 \text{ g}^{-1}$	$\langle R_g^2 \rangle^{1/2}/\text{nm}$
1	91.0	2.72	174.0	56.0
2	69.6	1.85	146.0	42.8
3	75.7	1.37	160.4	35.3
4	55.0	1.13	143.0	31.0
5	25.3	1.04	71.8	20.3
6	23.1	1.08	69.3	20.2
7	15.6	1.04	49.5	15.5
8	9.84	1.05	37.7	
9	9.80	1.08	36.9	
10	4.87	1.05	21.5	
11	2.07	1.03	11.6	
12	1.99	1.04	11.2	
13	1.70	1.05	10.5	
14	1.51	1.04	9.8	
15	1.13	1.04	8.2	
16	0.605	1.04	5.8	
17	0.374	1.07	4.4	
18	0.425	1.06	4.4	

chains and backbone, the fraction of side chains can be determined within each SEC slice. This has been tested by comparing the results of the UV analysis of defined mixtures of labeled and unlabeled poly(*p*-methylstyrene) with the charged amounts.

Results and Discussion

Linear Polymers. The calculation of contraction factors requires intrinsic viscosities or radii of gyration for linear polymers in order to compare the respective values with those of the branched polymer. Thus, a variety of linear poly(*p*-methylstyrene)s having broad and narrow molecular weight distributions were synthesized and analyzed with respect to their molecular weight averages, intrinsic viscosities, and mean-squared radii of gyration. For the samples having molecular weights of less than 10^5 g/mol, which revealed narrow peaks in the chromatograms the weight-average molecular weights, M_w , as determined from SEC-LS were assigned to the elution volumes of the peak maxima. For the higher molecular weight region, molecular weights for individual slices of the broad molecular weight samples were used for calibration purposes. A good agreement between the data obtained for the individual slices of a broad distributed sample and those from the narrowly distributed samples was found. The calibration curve obtained by this procedure was used for the final determination of molecular weight averages and polydispersities for the linear samples in a conventional way. Intrinsic viscosities were obtained from SEC viscosity detection upon integration over the complete peak. This procedure results in the weight-average intrinsic viscosity as it would be obtained from viscometry experiments using a capillary viscometer. The mean-squared radii were obtained from SEC-LS accordingly as z -averages for the complete peak. The characterization data for the linear samples are summarized in Table 1. The molecular weights cover the range from $10^3 < M < 10^6$ g/mol. Evaluation of the chromatograms using a polystyrene calibration curve results in molecular weights approximately 20% lower than those obtained from the poly(*p*-methylstyrene) calibration curve which is based on light scattering results. Beside the calibration curve, the dependences of intrinsic viscosity and radius of gyration on molecular weight were determined. Again narrowly distributed samples were used for the lower molecular weight region, while the results of individual SEC slices were

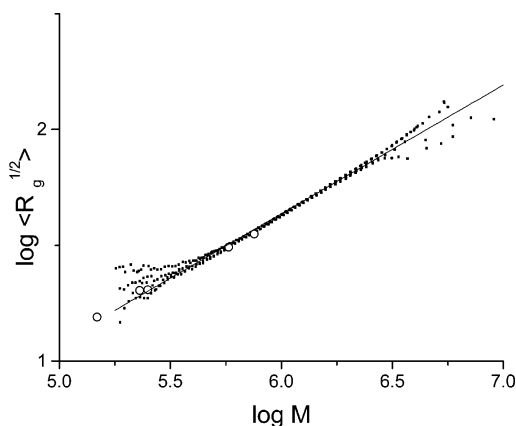


Figure 1. Dependence of root-mean-squared radius of gyration on molecular weight for poly(*p*-methylstyrene)s having narrow (○) and broad (●) molecular weight distribution. The solid line corresponds to the relationship $\langle R_g^2 \rangle^{1/2} = 18.4 \times 10^{-3} \text{ nm } M^{0.57}$.

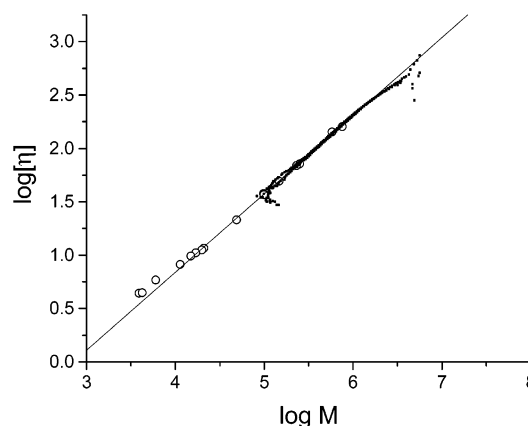


Figure 2. Mark-Houwink plot for poly(*p*-methylstyrene)s having narrow (○) and broad (●) molecular weight distribution. The solid line corresponds to $[\eta] = 8.3 \times 10^{-3} M^{0.731}$.

used for the higher molecular weight part. As can be seen from Figure 1 and Figure 2, the results obtained from the narrowly distributed samples agreed well with results obtained from the individual slices. The scaling behavior of the mean-squared radius with molecular weight was determined to be as

$$\langle R_g^2 \rangle^{1/2} = (18.4 \pm 2.3) \times 10^{-3} \text{ nm } M^{0.57 \pm 0.01}$$

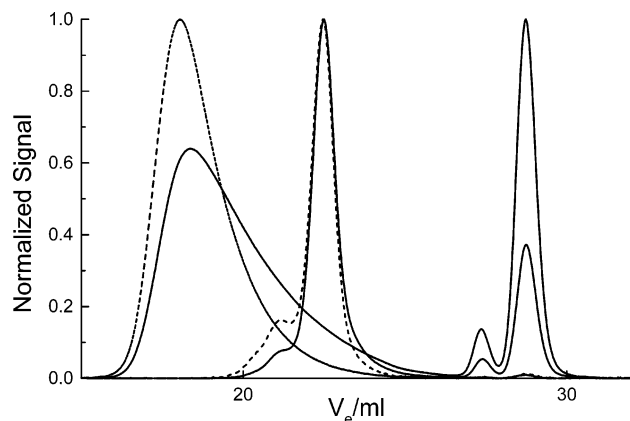
The exponent takes the value expected for a polymer coil in a good solvent.²² Comparison with the respective scaling behavior for polystyrene in THF³⁴ ($\langle R_g^2 \rangle^{1/2} = 13.9 \times 10^{-3} \text{ nm } M^{0.588}$) shows that the determined prefactor for poly(*p*-methylstyrene) is substantially higher than that of polystyrene. However, since the molecular weight dependence could be determined only over 1 decade of molecular weight, the extrapolation and therefore the prefactor should be regarded with caution.

The Mark-Houwink parameters were determined using the absolute molecular weights from light scattering and the intrinsic viscosities of the on-line viscosity detector. Only samples having molecular weights above 15×10^3 g/mol were used for this investigation, since for lower molecular weights the chains might be too short to be regarded as coils. In fact, as can be seen in Figure 2 in the lower molecular weight region the experimental data points are higher than the fitted line, indicating a different structure than for the higher

Table 2. Molecular Characteristics of Backbones (BB) and Side Chains (SC) Used for the Grafting-Onto Reactions

sample	code ^a	$M_n/10^3$	$M_w/10^3$	M_w/M_n	$[\eta]/\text{mL}^3 \text{g}^{-1}$	$\langle R_g^2 \rangle^{1/2}/\text{nm}$
BB1	●, ▲, ■	334	910	2.72	174	56
BB2	○, △, □	150	156	1.04	49.5	15.5
SC1	○, ●	3.50	3.74	1.07	4.4	
SC2	△, ▲	11.0	11.3	1.04	8.2	
SC3	□, ■	15.4	16.0	1.04	9.8	

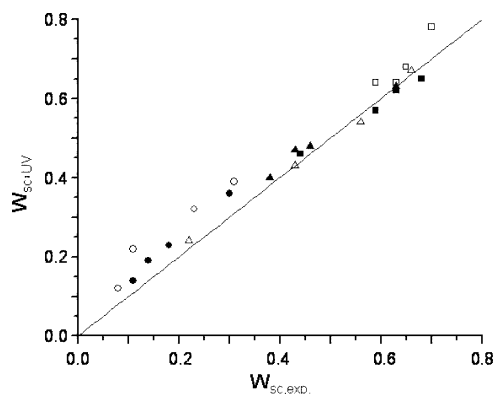
^a Solid symbols correspond to samples having a backbone with broad molecular weight distribution (BB1), and open symbols correspond to samples having a backbone with narrow molecular weight distribution (BB2). The side chains are differentiated by the type of symbols.

**Figure 3.** Typical chromatogram of graft product obtained by reacting narrow distributed side chains with broad and narrow distributed backbone polymers: solid lines, RI traces; dashed lines, 90° light scattering traces.

molecular weight part. The Mark–Houwink parameters were determined to be $a_\eta = 0.731$ and $K = 8.3 \times 10^{-3} \text{ mL/g}$, respectively. The scaling behavior resembles that for a coiled molecule in a good solvent. Taking into account only samples having broad molecular weight distribution, we end up specially with a considerable higher value of the Mark–Houwink parameter ($a_\eta = 0.717$, $K = 9.98 \times 10^{-3} \text{ mL/g}$), indicating again the problems associated with the extrapolation to zero molecular weight. Comparison with the Mark–Houwink relationship for polystyrene in THF³⁵ ($[\eta] = 13.14 \times 10^{-3} M^{0.714}$) indicates a lower intrinsic viscosity for poly(*p*-methylstyrene) at the same molecular weight.

Comb Polymers. Integral Properties. Comb polymers of poly(*p*-methylstyrene) were synthesized by the “grafting onto” strategy as described in the Experimental Part. The molecular characteristics of the linear polymers used for backbone and side chains are given in Table 2.

Typical chromatograms of the products of the grafting reactions are shown in Figure 3. A considerable amount of unreacted side chains can be observed at the low molecular weight end of the chromatogram. This is due to substantial side reactions like metal–halogen exchange and termination by protic impurities. Attempts to reduce this residual amount of precursors by more sophisticated purification procedures failed. The residual side chains would require tedious fractionation if characterization would have to be done by classical means, i.e., without SEC separation before light scattering or viscometric analysis. The introduction of the phenanthrene label results in a slightly different UV spectrum of the pure side chains as compared to pure

**Figure 4.** Comparison of the weight fraction of grafts obtained from UV analysis, $w_{\text{sc,UV}}$, and from the amounts of polymers charged during synthesis, $w_{\text{sc,exp}}$. For symbols, see Table 2. The solid line corresponds to $w_{\text{sc,UV}} = w_{\text{sc,exp}}$.

poly(*p*-methylstyrene). The integral composition can therefore be analyzed by means of UV analysis. Upon integration over the peak one obtains from eq 1

$$\frac{\Delta V \sum A_{c,i}(\lambda)}{m_{\text{inj}}} = [w_{\text{sc,UV}} \epsilon_{\text{sp,sc}}(\lambda) + (1 - w_{\text{sc,UV}}) \epsilon_{\text{sp,bb}}(\lambda)] \quad (2)$$

Here ΔV is the volume of a SEC slice and m_{inj} is the total mass injected. The data obtained from eq 2 can be compared with the amounts of side chains and backbone material charged during the grafting reaction ($w_{\text{sc,exp}}$). Figure 4 shows a good correlation between the two methods. Only for low fractions of side chains we observe stronger deviations. Undesired fractionation during the workup should result in too low a fraction of side chains in the UV analysis, while higher values are found. A significant change in the UV spectrum of the phenanthrene unit upon grafting to the backbone could be another explanation. However, model studies using phenanthrene-labeled poly(*p*-methylstyrene) anions which had been terminated with benzyl bromide showed no significant difference between the specific absorption of benzyl- and proton-terminated chains. A closer inspection of the crucial data points shows that the discrepancy exists only for the shortest side chains irrespective of the type of the backbone used. Since all grafting experiments with a certain side chain length have been carried out using the same solution of poly(*p*-methylstyrene) anions, it seems reasonable to assume that the discrepancy results from weighing errors during the synthesis of the poly(*p*-methylstyrene) with the lowest molecular weight.

In principle, it is also possible to derive the weight fraction of the side chains from light scattering data using

$$w_{\text{sc}} = 1 - \frac{M_{\text{n,bb}}}{M_{\text{n}}} \quad (3)$$

with $M_{\text{n,bb}}$ and M_{n} the number-average molecular weight of the backbone and the comb polymer, respectively. These values can be extracted from Table 2 and Table 3. In doing so, a good correlation between the results from the light scattering and from the UV analysis is observed, provided the combs were prepared using a backbone with low polydispersity. For combs

Table 3. Characterization Data of the Pure Comb Polymers

code ^e	100λ _{bb,calc} ^a	100λ _{bb,exp}	w _{sc,UV}	M _{w,LS} /10 ⁵ ^f	M _{w,LS} /M _{n,LS} ^g	(R _g ²) ^{1/2} /nm	[η] _w /cm ³ g ⁻¹
●	4.0	1.68	0.35	15.1	2.02	67	158
▲		1.55	0.59	20.6	2.00	71	159
■		1.37	0.64	23.5	2.03	73	160
●	2.0	0.69	0.18	11.7	2.00	62	161
▲		0.61	0.36	16.1	2.25	71	164
■		0.58	0.43	17.8	2.15	70	162
●	1.0	0.88	0.22	12.5	2.09	68	167
▲		0.72	0.40	15.0	1.98	63	166
■		0.63	0.45	14.5	2.01	64	181
●	0.5	0.47	0.13	12.3	2.09	66	179
▲		0.38	0.26	14.3	2.07	65	181
■		0.35	0.31	15.9	2.07	63	160
○	4.0 ^b	2.04	0.39	2.77	1.29		47
△		2.16	0.60	4.09	1.16		48
□		2.45	0.66	4.72	1.21		52
○	2.0 ^c	1.40	0.31	2.10	1.09		47
△		1.21	0.53	3.25	1.10		49
□		1.12	0.59	3.39	1.14		52
○	1.0 ^d	0.78	0.20	1.88	1.09		47
△		0.71	0.40	2.53	1.08		49
□		0.69	0.47	2.73	1.09		51
○	0.5	0.39	0.11	1.65	1.07		49
△		0.26	0.20	1.88	1.07		49
□		0.32	0.29	2.08	1.09		48

^a Calculated from reagents charged during bromination, i.e., molar ratio of [NBS]₀/[CH₃]₀ with [CH₃]₀ molar concentration of *p*-methyl groups in poly(*p*-methylstyrene). ^b λ_{bb} = 1.8% as determined by ¹H NMR. ^c λ_{bb} = 1.3% as determined by ¹H NMR. ^d λ_{bb} = 0.52% as determined by ¹H NMR. ^e Symbols as defined in Table 2. ^f M_{w,LS} = Σc_iM_i/Σc_i. ^g M_{n,LS} = Σc_i/Σc_i/M_i.

having a backbone with a broad molecular weight distribution significantly higher values for the weight fraction of the backbone were found by the light scattering approach. This is due to the reduced sensitivity of the light scattering instrument at the lower molecular weight tail of the chromatogram. It is often observed that even for linear polymers the number-average molecular weights obtained by SEC-LS are higher than from conventional SEC. Since the number-average molecular weight of the backbone is obtained from conventional SEC, while the number-average molecular weight of the comb from SEC-LS, this results in a too high fraction of material in the side chains when using eq 3.

By integration over the comb part only the average molecular weights, the intrinsic viscosities, and the mean-squared radii of gyration for the pure comb polymer can be determined. Knowing the weight fraction of material in the side chains, *w*_{sc}, and their number-average degree of polymerization, *P*_{n,sc}, it is possible to determine the grafting frequency, λ_{bb}, defined as the fraction of grafted backbone units.

$$\lambda_{bb} = \frac{m_{sc}/M_{n,sc}}{m_{bb}/M_0} = \frac{m_{sc}/P_{n,sc}}{m_{bb}} \quad (4)$$

$$\lambda_{bb} = \frac{w_{sc}}{P_{n,sc}(1 - w_{sc})} \quad (5)$$

Here *m*_{sc} and *m*_{bb} are the mass of the backbone and side chain, respectively, while *M*₀ is the molecular weight of a repeating unit.

The characterization data of the comb polymers are summarized in Table 3.

Results on Individual Slices. Beside the determination of average molecular weights of the complete sample, the use of light scattering and viscometry with SEC allows to obtain the same information for each eluting fraction.

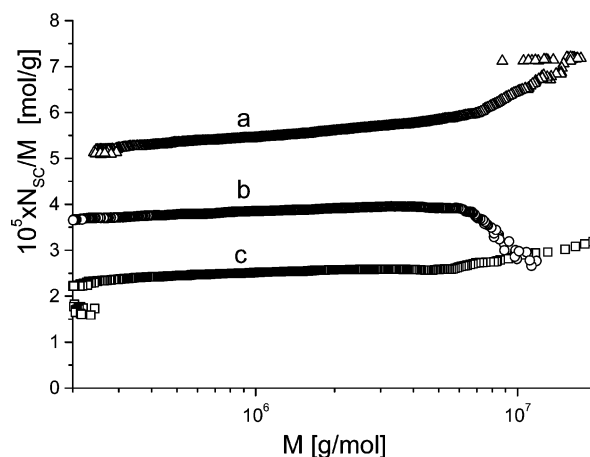


Figure 5. Number of side chains per molecular weight, *N*_{sc,*i*}/*M*_{*i*}, as a function of the molecular weight of the comb polymer. a (Δ): λ_{bb} = 1.68%; b (○): λ_{bb} = 0.72%; c (□): λ_{bb} = 0.38%; *M*_{n,sc} = 1.11 × 10⁴.

The number of side chains per comb molecule in a particular SEC slice, *N*_{sc,*i*}, is given by

$$N_{sc,i} = \frac{M_i w_{sc,i}}{M_{n,sc}} \quad (6)$$

Here *M*_{*i*} and *M*_{n,sc} are the molecular weight of the comb in the SEC slice and the number-average molecular weight of the side chains. *w*_{sc,*i*} is the weight fraction of the side chains in the SEC slice, as determined from UV analysis according to eq 1. The determination of the number of side chains in each SEC slice allows to detect variations of side chain distribution with molecular weight.

As an example, Figure 5 shows a plot of *N*_{sc,*i*}/*M*_{*i*} vs *M*_{*i*}. The number of side chains per molecular weight, which is proportional to the weight fraction of material in the side chains, increases slightly but significantly with the molecular weight of the comb. This slight

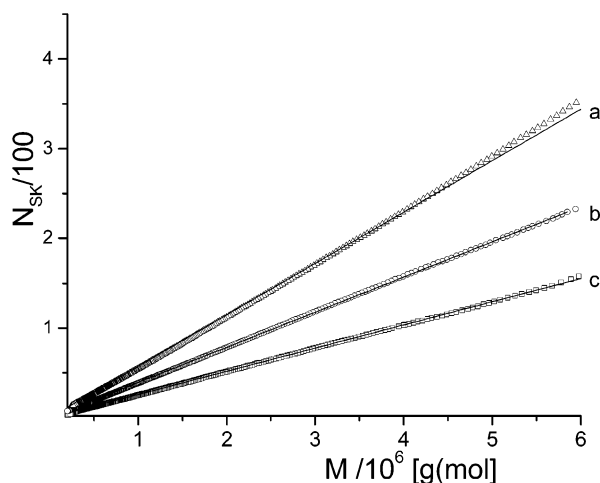


Figure 6. Number of side chains, $N_{sc,i}$, as a function of molecular weight of the comb polymer: \triangle , $\lambda_{bb} = 1.68\%$; \circ , $\lambda_{bb} = 0.72\%$; \square , $\lambda_{bb} = 0.38\%$; $M_{n,sc} = 1.11 \times 10^4$. The branching frequencies obtained by linear regression are $\lambda_{bb} = 1.89\%$, 0.84% , and 0.43% .

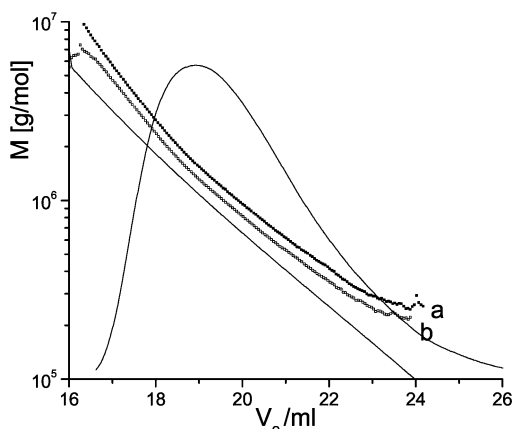


Figure 7. Comparison of SEC calibration curves for comb polymers with varying branching frequencies, having constant side chain molecular weight of 1.11×10^4 g/mol: \blacksquare , $\lambda_{bb} = 1.55\%$; \square , $\lambda_{bb} = 0.38\%$. For comparison, the calibration curve for linear poly(*p*-methylstyrene) is included. The chromatogram corresponds to the broad distributed backbone.

increase in the fraction of side chains with increasing molecular weight has been observed for nearly all samples, with the backbone having a broad molecular weight distribution.

Using the molecular weights of the individual SEC slices, which were obtained by SEC with light scattering detection, the number of side chains can be calculated as a function of the molecular weight of the comb polymer. It becomes clear from Figure 6 that the number side chains increases nearly linearly with molecular weight. The slight upward curvature is due to the slight increase in the weight fraction of side chains mentioned above. Up to several hundred side chains were attached for high molecular weight combs.

Molecular Weights. Figure 7 compares the SEC calibration curves for linear polymers and combs of varying branching frequencies but constant side chain length. Similar behavior is by found comparing the calibration curves at roughly constant branching frequency but varying side chain molecular weight. In general, a more or less parallel shift to higher molecular weights can be found, indicating the more compact structure of the comb polymers relative to the linear ones. In both cases

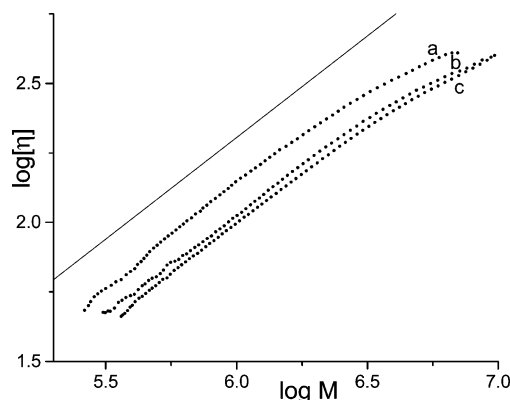


Figure 8. Comparison of Mark-Houwink relationships for comb polymers of varying branching frequencies, λ_{bb} , at constant side chain length, $M_{n,sc} = 1.11 \times 10^4$ g/mol: a, $\lambda_{bb} = 0.38\%$; b, $\lambda_{bb} = 0.72\%$; c, $\lambda_{bb} = 1.55\%$. The solid curve shows the Mark-Houwink relation for linear poly(*p*-methylstyrene) in THF.

the deviation from the calibration curve of the linear sample increases with the weight fraction of side chains. In fact, it has been found that the factor governing the shift of the calibration curve is weight fraction of side chains. This assumption is correct within an error of about 10%.¹⁷ The observed parallel shift of the calibration curves is a first indication that the power law for combs is not significantly different from the power law of the linear polymers. Finally, an upward curvature is observed at the high molecular weight end, which might be due to a slight column overloading.

Intrinsic Viscosities. Beside the absolute molecular weights obtained by SEC-MALLS, we obtained the intrinsic viscosities of the individual fraction from SEC-viscometry. Thus, we can derive the Mark-Houwink relations, which are given in Figure 8. The graph compares the effect of branching frequency at constant side chain length. Similar plots are obtained for the effect of side chain length at comparable branching frequency (not shown). As in the case of the calibration curves, we observe a slight curvature at high molecular weights, which again might be due to slight overloading effects. The comparisons of the Mark-Houwink plots show a pronounced decrease of the intrinsic viscosities relative to the linear polymer, in particular at higher branching frequency and longer side chains.

The derived Mark-Houwink exponents, a_η , for individual samples with broad molecular weight distribution are all found to be in the range of 0.67 ± 0.01 , which is slightly lower than the value found for the linear polymer ($a_\eta = 0.717$). This value indicates a coiled structure of the combs in solution. To determine the contraction factors g' for the complete sample, we calculated the weight-average intrinsic viscosities of the linear sample having identical molecular weight distribution according to

$$[\eta]_{w,l} = \sum w(M_i) [\eta]_l(M_i) = \sum w(M_i) K_l M_i^{a_{\eta,l}} \quad (7)$$

Here, $w(M_i)$ is the molecular weight distribution of the comb as determined by SEC-LS, while K_l and $a_{\eta,l}$ are the Mark-Houwink parameters for the linear poly(*p*-methylstyrene). The dependence of g' as a function of branching frequency and side chain molecular weight is depicted in Figure 9. It is observed that the data obtained for comb polymers having broad molecular weight distribution closely follow the dependence found

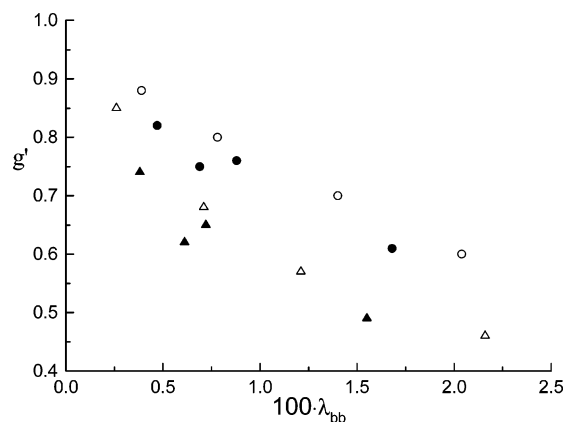


Figure 9. Dependence of contraction factor g' on branching frequency, λ_{bb} , for side chain length of $M_n = 3.74 \times 10^3$ g/mol (O, ●) and $M_n = 1.11 \times 10^4$ g/mol (Δ, ▲).

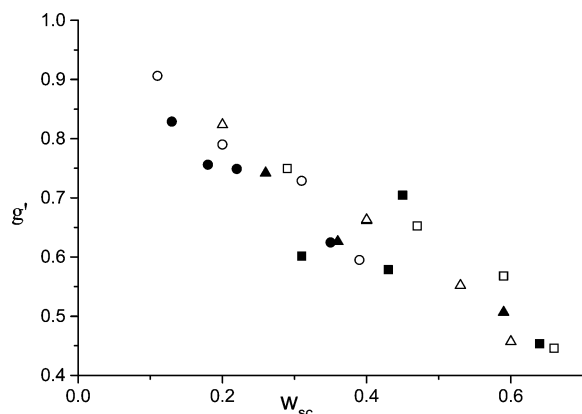


Figure 10. Dependence of contraction factor g' on weight fraction of material in the side chains, w_{sc} , for side chain length of $M_n = 3.74 \times 10^3$ g/mol (O, ●), $M_n = 1.11 \times 10^4$ g/mol (Δ, ▲), and $M_n = 1.54 \times 10^4$ g/mol (■, □).

for samples having narrow molecular weight distribution, despite some larger scattering of the former. Apparently, the introduction of a small amount of side chains is sufficient for a pronounced decrease of the intrinsic viscosity. To elucidate the effect of side chain length at a constant branching frequency, g' values for $\lambda_{bb} = 1.37\%$, 0.63% , and 0.35% were extracted from Figure 9. These values correspond to the experimentally determined branching frequencies for the side chain length of 1.54×10^4 g/mol. The so-obtained g' values have been compared as a function of side chain length (not shown). Regardless of the scatter, it became clear that even a small side chain molecular weight at a given branching frequency is enough to reduce the intrinsic viscosity significantly. A limiting value seems to be approached as the molecular weight of side chains increases. This limiting value for high side chain molecular weights is a function of the branching frequency.

A certain weight fraction of material can be incorporated into the side chains either by grafting a large number of short or by grafting only a few long side chains onto the backbone. Figure 10 shows the dependence of g' on the weight fraction of material in the side chains. A good linear correlation is observed with only negligible dependence of side chain length. This indicates that the reduction of intrinsic viscosity is a function of only the weight fraction of material in the side chains. A linear dependence of g' on the fraction of material in the backbone has also been found by Graessley on short-chain branched polyolefins.³⁶ Ac-

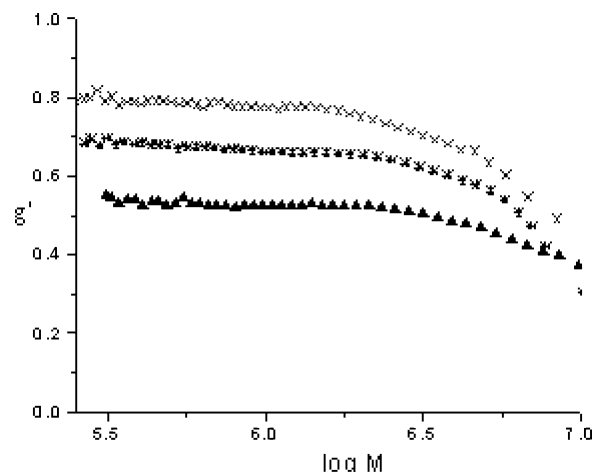


Figure 11. Dependence of g' on molecular weight of the comb polymer for side chain length of $M_n = 1.11 \times 10^4$ g/mol and various branching frequencies: x, $100 \lambda_{bb} = 0.38$; *, $100 \lambda_{bb} = 0.72$; ▲, $100 \lambda_{bb} = 1.55$.

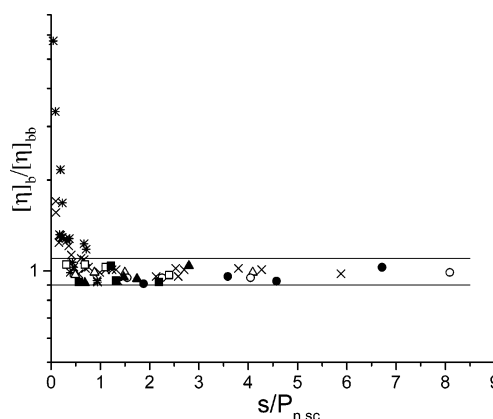


Figure 12. Comparison of the intrinsic viscosities of comb and parent backbone polymers (g'') as a function of the side chain distance, s , to side chain length, $P_{n,sc}$: x, *, literature data,^{37,38} for other symbols see Table 2.

cording to Cassasa and Berry, for a large number of side chains the branching ratio g of combs is expected to depend on the weight fraction of the backbone only.⁴ Figure 11 compares the dependences of the contraction factor g' on the molecular weight of the comb as a function of branching frequency for individual SEC slices. The contraction factor g' is nearly independent of the molecular weight of the comb polymer but decreases with increasing branching frequency, λ_{bb} , at constant side chain molecular weight. The slight downward curvature with increasing overall molecular weight is consistent with the assumption of slight column overloading as already discussed above. Similar results are obtained for the dependence on side chain molecular weight (not shown).

An interesting result is obtained by calculating the ratio $g'' = [\eta]_{br}/[\eta]_{bb}$ where $[\eta]_{bb}$ is the intrinsic viscosity of the backbone. Figure 12 shows the dependence of g'' on the ratio of the side chain distance, s , to the side chain length, $P_{n,sc}$. The average distance between the side chains was calculated using

$$s = \frac{M_{n,bb}}{N_{sc}} \quad (8)$$

It can be seen that the intrinsic viscosity of the comb is

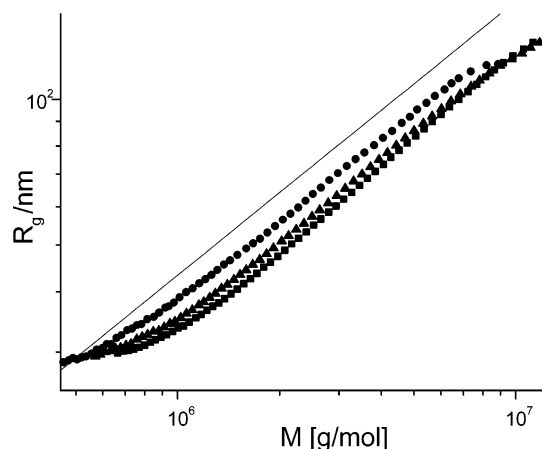


Figure 13. $\langle R_g^2 \rangle^{1/2}$ vs comb molecular weight, M , for comb polymers having comparable branching frequency but different side chain molecular weights: (●) $M_{n,sc} = 3.74 \times 10^3$ g/mol, $\lambda_{bb} = 1.68\%$; (▲) $M_{n,sc} = 1.11 \times 10^4$ g/mol, $\lambda_{bb} = 1.55\%$; (■) $M_{n,sc} = 1.54 \times 10^4$ g/mol, $\lambda_{bb} = 1.3\%$.

very close to the intrinsic viscosity of the parent backbone despite the significant higher molecular weights of the comb polymers. The increase in viscosity of the comb is limited to approximately 5%. Only if the distance between the side chains becomes smaller than the side chain length, i.e., the structure changes from comblike to a starlike, does the intrinsic viscosity of the comb increase significantly over that of the backbone. Thus, for comb polymers the contraction effect due to branching is compensated by coil expansion in such a way that the segment density stays nearly the same. Similar observations are described by Roovers, who also found only a very weak increase in intrinsic viscosity despite a 2.5-fold increase in molecular weight for polystyrene combs in toluene.^{37,38}

Mean-Squared Radii of Gyration. Using SEC equipped with multiangle light scattering detection, it is possible to determine the mean-squared radii for the individual SEC fractions, provided the sizes of the molecules are sufficiently large. Figure 13 shows the dependences of the root-mean-squared radii on comb molecular weight for different side chain molecular weights at comparable branching frequencies. Similar curves were obtained for the dependence on branching frequencies at constant side chain molecular weight. Similar to the results on the intrinsic viscosities, the mean-squared radii of the combs are substantially lower than those of the linear sample. The curves are more or less shifted parallel with respect to the curve of the linear molecule. The exponents of the power law are found to be within the range 0.52–0.55, again indicating the structure of coiled molecules in solution. This is in agreement with the power law found for the intrinsic viscosity. Similar exponents for the power laws of combs and linear polymers have also been found by MC simulations.^{19,20} The dependences of the radius of gyration on side chain length and branching frequency are similar to the data on intrinsic viscosity. The molecular weight range covered is smaller than for the intrinsic viscosity due to the limitations of light scattering, which allows reasonable determination of mean-squared radii only if the radii are sufficiently high, i.e., $R_g \geq 20$ nm. In accordance with the parallel shift of the R_g – M curves, the contraction factors $g = \langle R_{g,br}^2 \rangle / \langle R_{g,l}^2 \rangle$ do not vary strongly with molecular weight (not shown), similar to the g' values.

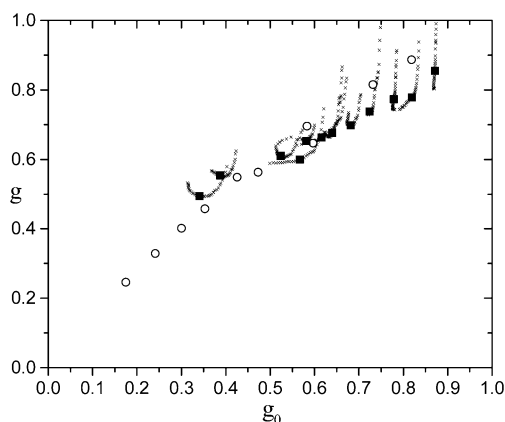


Figure 14. Dependence of g on g_0 . For slice data of combs having broad molecular weight distribution (×). ■, slices corresponding to $M_i = M_w$. For comparison, the literature data of Roovers^{37,38} are included (○).

Comparison with Theoretical Predictions. Casassa and Berry calculated g values for combs based on Gaussian chain approximation.⁴ Their result is given in eq 9

$$g_0 = (1 - w_{sc}) + \frac{2}{N_{sc}} w_{sc}^2 (1 - w_{sc}) + \left(\frac{3N_{sc} - 2}{N_{sc}^2} \right) w_{sc}^3 \quad (9)$$

Here, N_{sc} is the number of side chains and w_{sc} is the weight fraction of side chains. In the following discussion, g_0 denotes the calculated value derived under the assumption of Gaussian chains in order to differentiate from experimental data obtained under good solvent conditions (g). For high numbers of side chains eq 9 can be approximated by

$$g_0 = 1 - w_{sc} \quad (10)$$

The use of light scattering and viscosity detection seems to be a convenient way to compare the theoretically derived equations with experiment.

Since the determination of mean-squared radii of gyration by light scattering is restricted to molecules with sufficiently high molecular weights, it is often convenient for lower molecular weights to calculate the mean-squared radii from viscosity measurements using the Flory–Fox relation

$$[\eta] = \frac{6^{3/2} \Phi \langle R_g^2 \rangle^{3/2}}{M} \quad (11)$$

where Φ is the Flory constant which has a value of $2.86 \times 10^{23} \text{ mol}^{-1}$. Assuming the Flory constant to be independent of topology, the use of the Flory–Fox equation results in

$$g = \left(\frac{[\eta]_{br}}{[\eta]_l} \right)^{2/3} = (g')^{2/3} \quad (12)$$

In the following we will keep the terminology $(g')^{3/2}$ to differentiate between values obtained from viscosity measurements based on the Flory–Fox equation and g values based on the radii from light scattering.

Figure 14 and Figure 15 show the experimentally determined values of g and $(g')^{3/2}$ vs g_0 . The experimental data points for the SEC slices of a particular sample

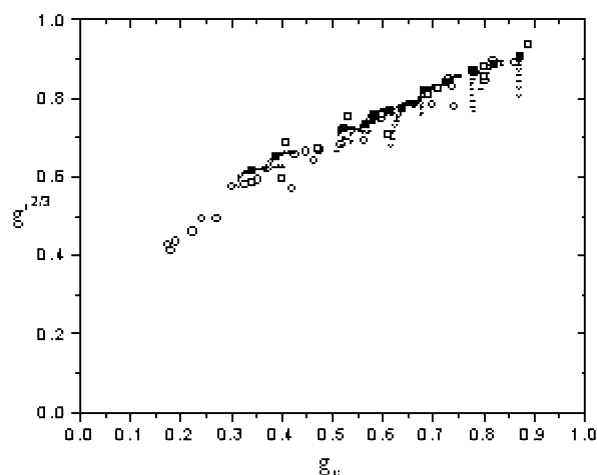


Figure 15. Relation between $(g')^{2/3}$ and g_0 for slice evaluation of comb polymers having broad molecular weight distribution (\times): \blacksquare , slices corresponding to $M_i = M_w$; \square , combs having narrow molecular weight distribution, this work. For comparison, the literature data of Roovers^{37,38} are included (\circ).

show substantial curvature. This is due to the experimental errors. The errors in g_0 reflect the errors in the determination of the slice composition by UV analysis, while the errors associated with the determination of g and g' are influenced by the errors associated with the determination of the mean-squared radius of gyration, intrinsic viscosity, and the molecular weights of the SEC slices. However, the central curves correspond to the central parts of the parts of the chromatograms and should contain the most valuable information. Therefore, information for selected SEC-slices in the center of the chromatogram are included in Figures 14 and 15. The slices have been selected such that the molecular weight of the slice, M_i , is identical to the weight-average molecular weight of the polydisperse comb, $M_{w,LS}$, given in Table 3. For comparison, literature data of Roovers^{37,38} on well-defined polystyrene combs have also been included. The values of Roovers and our data are close to each other, indicating that the results obtained from samples having broad molecular weight distribution using SEC with light scattering and viscometry detection produces similar results than experiments on carefully fractionated samples with narrow molecular weight distribution. However, the effort is substantially decreased for the former procedure.

The comparison of the theoretically expected g_0 with the experimentally obtained g or $(g')^{3/2}$ values reveals systematically higher g and $(g')^{3/2}$ values, with the deviation becoming stronger with increasing fraction of materials in the side chains, i.e., with decreasing g_0 (Figures 14 and 15). This seems to indicate a pronounced coil expansion of the comb relative to the linear polymer as a result of the increasing segment density of the comb. The calculation of g_0 does not include excluded-volume effects, while in the good solvents used for SEC experiments the excluded volume is pronounced. The observation differs, however, from the experimental results on star-shaped polymers where the g values found in good solvents do agree well with g_0 . The present results clearly show that the result for star-shaped polymers are due to a fortunate canceling of different effects, which will not be valid for all branched species. The observation that the relative dimensions of star polymers and comb polymers are changed to a different degree are in agreement with computer simu-

lations, where the mean-squared radii of stars in good solvents are found to be close to the Gaussian values, while combs show a clearly stronger expansion.^{11–14,18–20} Also, simulated SEC distribution coefficients of stars relative to linear molecules are not changed when going from random walks (Gaussian chains) to self-avoiding chains (good solvents) in contrast to combs, where the calibration curves for combs are shifted to lower distribution coefficients relative to linear chains, with increasing solvent quality.^{15,17}

In addition, the comparison of Figures 14 and 15 shows that the assumption $(g')^{3/2} = g'$, which results from the Flory–Fox equation, apparently is not fulfilled, since the deviations from the lines corresponding to $(g')^{2/3} = g_0$ and $g = g_0$ are different. Since the Flory–Fox equation is obtained using the assumption of Gaussian chains, this discrepancy might be attributed to excluded-volume effects. If this would be the case, application of the Ptitsyn–Eizner³⁹ approach might lead to a better agreement. The Ptitsyn–Eizner approach modifies the Flory–Fox equation by allowing the Flory constant to vary with solvent quality. The influence of solvent quality is accomplished via a dependence of the Flory–Fox parameter on the Mark–Houwink exponent, a_η .

$$\phi = \phi_0(1 - 2.63\epsilon + 2.86\epsilon^2) \quad (13)$$

$$\epsilon = \frac{2a_\eta - 1}{3} \quad (14)$$

Assuming that this approach is valid for linear as well as for branched species, we end up with

$$g'^{2/3} = \left(\frac{[\eta]_{br}}{[\eta]_l} \right)^{2/3} = \left(\frac{\phi_{br}}{\phi_l} \right)^{2/3} g \quad (15)$$

where the modified Flory parameters can be calculated from the respective Mark–Houwink exponents of the branched and linear species. In our investigations the average Mark–Houwink exponent is $a_\eta = 0.67$ for combs while for the linear poly(*p*-methylstyrene) a Mark–Houwink exponent of $a_\eta = 0.73$ was found. According to eq 15, this should result in a 5% increase of $(g')^{2/3}$ with respect to g . This increase should be nearly independent of the fraction of side chains, which is not the case in our experiments. Thus, the Ptitsyn–Eizner approach cannot account properly for the increasing deviations from the theoretical behavior with increasing side chain fraction of the comb. Berry and Orofino⁴⁰ calculated the effect of comb polymer expansion on g due to the excluded volume in good solvents. However, our attempts to correct for polymer coil expansion (not shown) using the equations given were also not successful. For the determination of branching in polymers the use of viscosity detectors is therefore complicated by the fact that equations relating molecular structure to size information are mainly based on the calculation of radii of gyration rather than on the calculation of intrinsic viscosity. On the other hand, viscosity detectors allow covering also regions of lower molecular weight or smaller sizes, for which light scattering detectors cannot yield mean-squared radii with sufficient accuracy. It is therefore interesting to correlate g ratios obtained from light scattering with g' ratios obtained from viscometry. The use of the Flory–Fox⁷ relation assuming the Flory parameter to be independent of branching results in $g' = g^{3/2}$. Zimm and Kilb, however,

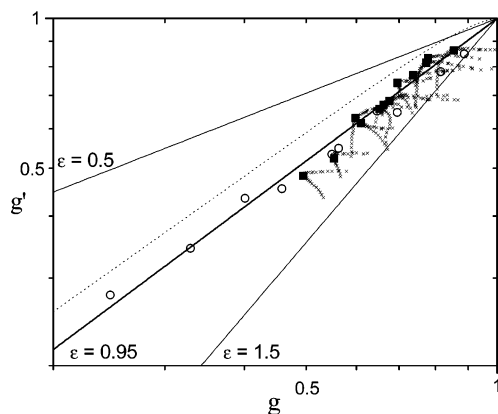


Figure 16. Relation between g' and g for poly(*p*-methylstyrol) combs having a broad molecular weight distribution (\times). (■) Slices corresponding to $M_i = M_w$. For comparison, the literature data of Roovers^{37,38} are included (*). Solid lines correspond to the equation $g' = g^\epsilon$, with values $\epsilon = 0.5, 0.95$, and 1.5 . The broken line corresponds to the relationship given in eq 16.

derived $g' = g^{1/2}$ for star polymers⁸ and assumed this relationship to be universal. Berry^{2,9} suggested a structure-dependent value of the exponent ϵ , which varies with the fraction of material in the side chains. According to his assumption ϵ changes from a value close to 0.44 for starlike structures to a value of approximately 1 for combs. Until today, the discussion on the correct value of the exponent ϵ in the relation $g' = g^\epsilon$ continues. On the basis of a large number of experimental data on star polymers, the following empirical formula was derived by Burchard:

$$g' = (a + (1 - a)g^p)g^b \quad (16)$$

with $a = 1.104$, $p = 7$, and $b = 0.906$.

The correlation between g and g' can be deduced by application of SEC equipped with both light scattering and viscometry detector. Figure 16 shows the relationship between g and g' for the comb polymers investigated. It becomes clear that neither the Flory–Fox approach nor the Zimm–Kilb relation or the empirical approach for stars (eq 16) is suitable to describe the experimental data of the combs under investigation. Because of the scattering of the data, which is the result of different sources of uncertainty in the experiments, a simple linear fit to all of the data on the slices would not be appropriate. We therefore have used only the selected slices in the center of the chromatograms for fitting the exponent ϵ . The use of these data results in a value of $\epsilon = 0.95$. This finding is also in agreement with literature data on monodisperse combs, which are also given in Figure 16 and with the corresponding data on star polymers.⁴¹ Hama et al.⁴² found $\epsilon = 1$ for fractions of randomly branched polyolefins. Using the approximations of Berry⁹ and keeping in mind the large number of side chains, ϵ should vary between 0.54 and 1.1 for g values of 0.5 and 0.9, respectively. However, because of the scattering of our data, such a variation of ϵ cannot be detected.

Despite the common assumption of the Flory–Fox parameter to be independent of structure, the factor depends on the hydrodynamic interaction of the segments and therefore on their average distance, which in branched polymers is lower as compared to linear molecules. Consequently, the Flory parameter of a branched molecule, Φ_b , will be higher than the one of linear chains, Φ_l . Therefore

$$[\eta]_b = \Phi_b \left(\frac{R_{g,b}^2}{M} \right)^{3/2} > \Phi_l \left(\frac{R_{g,b}^2}{M} \right)^{3/2}$$

$$g' = \frac{\Phi_b \left(\frac{R_{g,b}^2}{M} \right)^{3/2}}{\Phi_l \left(\frac{R_{g,l}^2}{M} \right)^{3/2}} > \left(\frac{R_{g,b}^2}{R_{g,l}^2} \right)^{3/2} = g^{3/2} \quad (17)$$

The result $g' > g^{3/2}$ is clearly verified in Figure 16. However, the interpretation of the data is complicated by the fact that the present results are obtained under good solvent conditions. Thus, the effect of excluded volume, as discussed above when comparing g and g_0 , and the effect of the dependence of the Flory parameter on branching cannot be separated from each other.

To determine properly the amount of branches in comb polymers by SEC-LS or SEC-viscometry, we cannot use the equations based on Gaussian chain statistics. We rather have to use empirical relations. A useful approach is given by the fact that the intrinsic viscosities of the comb polymer and that of the parent backbone polymer are equal within a 10% accuracy limit (Figure 12). From the relation $[\eta]_{br} \approx [\eta]_{bb}$ we derive

$$[\eta]_{br} = KM_{bb}^\alpha = KM_b^\alpha (1 - w_{sc})^\alpha \quad (18)$$

from which the fraction of side chains is readily estimated.

Conclusion

SEC equipped with light scattering and viscometry detector is a powerful tool for the investigation of branched structures. The results obtained are comparable to the results obtained on narrow distributed samples synthesized by controlled polymerization techniques. It has been found that comb polymers show the same exponents on the power laws as linear coil molecules in solution. The extraction of the number of branches from size information is questionable due to a lack of theory predicting quantitatively the sizes in good solvents. Quantitative values might be obtained in easier ways by using empirical relations, which can be obtained using suitable branched structures. These, however, have to allow for independent branching characterization rather than to have narrow molecular weight distributions. As an example, we found the relationship $[\eta]_b \approx [\eta]_{bb}$ useful for comb polymers. We furthermore found for comb polymers a value close to $\epsilon = 1$ suitable in the relationship $g' = g^\epsilon$.

Acknowledgment. The authors thank Mrs. Christine Rosenauer (Max Planck Institute of Polymer Science, Mainz) for performing static light scattering measurements and for determining the refractive index increment of poly(*p*-methylstyrene).

References and Notes

- (1) Zimm, B. H.; Stockmayer, W. H. *J. Chem. Phys.* **1949**, *17*, 1301.
- (2) Berry, G. C. *J. Polym. Sci., Part A-2* **1968**, *6*, 1551.
- (3) Kurata, M.; Fukatsu, M. *J. Chem. Phys.* **1964**, *41*, 2934.
- (4) Casassa, E. F.; Berry, G. C. *J. Polym. Sci., Part A-2* **1966**, *4*, 881.
- (5) Radke, W.; Müller, A. H. E. *Macromol. Theory Simul.* **1996**, *5*, 759.
- (6) Burchard, W. *Adv. Polym. Sci.* **1983**, *48*, 4.
- (7) Flory, P. J. *Principles of Polymer Chemistry*, 16th ed.; Cornell University Press: Ithaca, NY, 1986.
- (8) Zimm, B. H.; Kilb, R. W. *J. Polym. Sci.* **1959**, *37*, 19.
- (9) Berry, G. *J. Polym. Sci., Part B: Polym. Phys.* **1988**, *26*, 1137.

- (10) Zifferer, G. *Makromol. Chem., Theory Simul.* **1993**, 2, 653.
(11) Zifferer, G. *Makromol. Chem.* **1991**, 192, 1555.
(12) Zifferer, G. *Makromol. Chem., Theory Simul.* **1994**, 3, 163.
(13) Gallacher, L. V.; Windwer, S. *J. Chem. Phys.* **1966**, 44, 1139.
(14) Zifferer, G. *Makromol. Chem., Theory Simul.* **1992**, 1, 55.
(15) Radke, W. *Macromol. Theory Simul.* **2001**, 10, 668.
(16) Radke, W.; Gerber, J.; Wittmann, G. *Polymer* **2003**, 44, 519.
(17) Radke, W. *J. Chromatogr. A* **2004**, 1028/2, 211.
(18) McCrackin, F. L.; Mazur, J. *Macromolecules* **1981**, 14, 12154.
(19) Lipson, J. E. G. *Macromolecules* **1991**, 24, 1327.
(20) Lipson, J. E. G. *Macromolecules* **1993**, 26, 203.
(21) Zifferer, G. *Makromol. Chem.* **1990**, 191, 2717.
(22) Wintermantel, M.; Schmidt, M.; Becker, A.; Dorn, R.; Kühn, A.; Lösch, R. *Nachr. Chem. Technol. Lab.* **1992**, 40, 331.
(23) Wyatt, P. J. *Anal. Chim. Acta* **1993**, 272, 1.
(24) Yau, W. W. *Chemtracts, Macromol. Chem.* **1990**, 1, 1.
(25) Ouano, A. C. *J. Appl. Polym. Sci., Part A-1* **1972**, 10, 2169.
(26) Haney, M. A. *J. Appl. Polym. Sci.* **1985**, 30, 3037.
(27) Haney, M. A. *J. Appl. Polym. Sci.* **1985**, 30, 3023.
(28) Haney, M. A. *Am. Lab.* 1985.
(29) Benoît, H.; Grubisic, Z.; Rempp, P.; Decker, D.; Zilliox, J. G. *J. Chem. Phys.* **1966**, 63, 1507.
(30) Hruska, Z.; Vuillemin, B.; Riess, G.; Katz, A.; Winnik, M. A. *Macromol. Chem.* **1992**, 193, 1987.
(31) Radke, W. Thesis, Mainz, 1996.
(32) Value selected by Wytatt Technology Astra, Version 4.02.
(33) Berkowitz, S. A. *J. Liq. Chromatogr.* **1983**, 6, 1359.
(34) Schulz, G. V.; Baumann, H. *Makromol. Chem.* **1968**, 114, 122.
(35) Meyerhoff, G.; Appelt, B. *Macromolecules* **1979**, 12, 968.
(36) Sun, T.; Brant, P.; Chance, R. R.; Graessley, W. W. *Macromolecules* **2001**, 34, 6812.
(37) Roovers, J. E. L. *Polymer* **1975**, 16, 827.
(38) Roovers, J. *Polymer* **1979**, 20, 843.
(39) Ptitsyn, O. B.; Eizner, Y. E. *J. Chem. Phys. (USSR)* **1959**, 29, 1117.
(40) Berry, G. C.; Orofino, T. A. *J. Chem. Phys.* **1964**, 40, 1614.
(41) Burchard, W. *Adv. Polym. Sci.* **1999**, 143, 113.
(42) Hama, T.; Yamaguchi, K.; Suzuki, T. *Makromol. Chem.* **1972**, 155, 283.

MA047799+